

Growth, characterization, and Raman spectra of the 1*T* phases of $TiTe_2$, $TiSe_2$, and TiS_2

Xiao-Fang Tang(唐筱芳), Shuang-Xing Zhu(朱双兴), Hao Liu(刘豪), Chen Zhang(章晨), Qi-Yi Wu(吴旗仪), Zi-Teng Liu(刘子腾), Jiao-Jiao Song(宋姣姣), Xiao Guo(郭晓), Yong-Song Wang(王永松), He Ma(马赫), Yin-Zou Zhao(赵尹陬), Fan-Ying Wu(邬钒颖), Shu-Yu Liu(刘姝妤), Kai-Hui Liu(刘开辉), Ya-Hua Yuan(袁亚华), Han Huang(黄寒), Jun He(何军), Wen Xu(徐文), Hai-Yun Liu(刘海云), Yu-Xia Duan(段玉霞), and Jian-Qiao Meng(孟建桥)
Citation: Chin. Phys. B, 2022, 31 (**3**): 037103. DOI: 10.1088/1674-1056/ac306a
Journal homepage: http://cpb.iphy.ac.cn; http://iopscience.iop.org/cpb

What follows is a list of articles you may be interested in

Pressure- and temperature-dependent luminescence from Tm^{3+} ions doped in $GdYTaO_4$

Peng-Yu Zhou(周鹏宇), Xiu-Ming Dou(窦秀明), Bao-Quan Sun(孙宝权), Ren-Qin Dou(窦仁琴), Qing-Li Zhang(张庆礼), Bao Liu(刘鲍), Pu-Geng Hou(侯朴赓), Kai-Lin Chi(迟凯鄰), and Kun Ding(丁琨)
Chin. Phys. B, 2022, 31 (**1**): 017101. DOI: 10.1088/1674-1056/ac0526

Review of Raman spectroscopy of two-dimensional magnetic van der Waals materials

Yu-Jia Sun(孙宇伽), Si-Min Pang(庞思敏), and Jun Zhang(张俊)
Chin. Phys. B, 2021, 30 (**11**): 117104. DOI: 10.1088/1674-1056/ac1e0f

Polarization-resolved Raman spectra of α -PtO_2

Zhanhong Lei(雷展宏), Weiliang Wang(王伟良), and Juncong She(佘峻聪)
Chin. Phys. B, 2021, 30 (**4**): 047102. DOI: 10.1088/1674-1056/abccb5

Direct observation of melted Mott state evidenced from Raman scattering in 1T-TaS_2 single crystal

Qing Hu(胡庆), Cong Yin(尹聪), Leilei Zhang(张雷雷), Li Lei(雷力), Zhengshang Wang(王正上), Zhiyu Chen(陈志禹), Jun Tang(唐军), Ran Ang(昂然)
Chin. Phys. B, 2018, 27 (**1**): 017104. DOI: 10.1088/1674-1056/27/1/017104

Homopolar bonds in Se-rich Ge—As—Se chalcogenide glasses

Si-Wei Xu(许思维), Rong-Ping Wang(王荣平), Zhi-Yong Yang(杨志勇), Li Wang(王丽), Luther-Davies Barry
Chin. Phys. B, 2016, 25 (**5**): 057105. DOI: 10.1088/1674-1056/25/5/057105

Growth, characterization, and Raman spectra of the 1*T* phases of $TiTe_2$, $TiSe_2$, and TiS_2

Xiao-Fang Tang(唐筱芳)[1,2,3], Shuang-Xing Zhu(朱双兴)[3,†], Hao Liu(刘豪)[3], Chen Zhang(章晨)[3], Qi-Yi Wu(吴旗仪)[3], Zi-Teng Liu(刘子腾)[3], Jiao-Jiao Song(宋姣姣)[3], Xiao Guo(郭晓)[3], Yong-Song Wang(王永松)[3], He Ma(马赫)[4], Yin-Zou Zhao(赵尹陬)[3], Fan-Ying Wu(邬钒颖)[3], Shu-Yu Liu(刘姝妤)[3], Kai-Hui Liu(刘开辉)[4], Ya-Hua Yuan(袁亚华)[3], Han Huang(黄寒)[3], Jun He(何军)[3], Wen Xu(徐文)[1], Hai-Yun Liu(刘海云)[5], Yu-Xia Duan(段玉霞)[3], and Jian-Qiao Meng(孟建桥)[3,‡]

[1] *Key Laboratory of Materials Physics, Institute of Solid State Physics, Chinese Academy of Sciences, Hefei* 230031, *China*
[2] *University of Science and Technology of China, Hefei* 230026, *China*
[3] *School of Physics and Electronics, Central South University, Changsha* 410083, *China*
[4] *State Key Laboratory for Mesoscopic Physics, Collaborative Innovation Center of Quantum Matter, School of Physics, Peking University, Beijing* 100871, *China*
[5] *Beijing Academy of Quantum Information Sciences, Beijing* 100085, *China*

(Received 20 August 2021; revised manuscript received 11 October 2021; accepted manuscript online 18 October 2021)

High-quality large 1*T* phase of TiX_2 (X = Te, Se, and S) single crystals have been grown by chemical vapor transport using iodine as a transport agent. The samples are characterized by compositional and structural analyses, and their properties are investigated by Raman spectroscopy. Several phonon modes have been observed, including the widely reported A_{1g} and E_g modes, the rarely reported E_u mode (~183 cm^{-1} for $TiTe_2$, and ~185 cm^{-1} for TiS_2), and even the unexpected K mode (~85 cm^{-1}) of $TiTe_2$. Most phonons harden with the decrease of temperature, except that the K mode of $TiTe_2$ and the E_u and "A_{2u}/Sh" modes of TiS_2 soften with the decrease of temperature. In addition, we also found phonon changes in $TiSe_2$ that may be related to charge density wave phase transition. Our results on TiX_2 phonons will help to understand their charge density wave and superconductivity.

Keywords: transition-metal dichalcogenides, chemical vapor transport, Raman, phonon

PACS: 71.45.Lr, 63.20.D–, 81.10.Bk **DOI:** 10.1088/1674-1056/ac306a

Following the discovery of graphene, layered transition-metal dichalcogenides (TMDCs) with the chemical formula TX_2 (T: transition metal; X: chalcogen) have attracted more attention. The quasi-two-dimensional (2D) TMDCs, attracted by relatively weak van der Waals-like forces, have rich physical properties such as topological superconductivity (SC),[1,2] charge density wave (CDW),[3,4] extremely large magnetoresistance,[5] and Dirac semimateal.[6,7] Due to the weak interaction between layers, it is possible for TMDCs materials to break the dimension limit and realize the application of few layers,[8] or even monolayer devices.[9,10]

Titanium disulphides (TiX_2, X = Te, Se, and S) are typical representatives of TMDCs. They have been studied extensively for their fascinating properties and potential applications. $TiTe_2$[11–13] and $TiSe_2$[14–16] are typical semimetals. Most researchers consider TiS_2 to be a semiconductor,[17,18] but some consider it to be semimetal.[19] 1*T*-$TiTe_2$ has been considered as a textbook Fermi liquid system.[20] CDW and SC have been confirmed in both $TiTe_2$[4,21,22] and $TiSe_2$.[23–27] Bulk $TiSe_2$ undergoes a CDW phase transition at 202 K,[28,29] and that of the monolayer $TiSe_2$ increased to over 232 K.[25–27] Recently, CDW phase transition has been revealed in single-layer $TiTe_2$ samples at 92 ± 3 K,[4] while no CDW has been found in bulk $TiTe_2$. For TiS_2, theoretical calculation suggests that CDW and SC can be tuned by doping.[30] 1*T* phases of $TiTe_2$[21,31,32] and $TiSe_2$[33] have been suggested as possible candidates for exploring topological SC. In TMDCs compounds, both CDW and SC are considered to be closely related to phonons.[21,30,34] The systematic study of phonon properties in TiX_2 is helpful to understand CDW and SC better.

High-quality large-size single crystals of TiX_2 were grown utilizing the chemical vapor transport method. Ti (99.99%, powder) and X (99.99%, powder) was mixed with a molar ratio of 1:2. Iodine (99.95%, powder) was used as the transport agent. We found that the growth of TiX_2 single crystals depends closely on many parameters, such as mixture heating temperature, crystal growth temperature, temperature gradient, growth time, and iodine concentration. We have tried different conditions, and the following parameters were applied to obtain high-quality large-size TiX_2 crystals. The mixture was sealed into quartz tubes in a vacuum (10^{-3} Torr, 1 Torr = 1.33322×10^2 Pa) and placed in a two-zone furnace, and then heated to specified temperatures for nearly two weeks. For the growth of $TiTe_2$, the mixture at one end was

†Corresponding author. E-mail: 182211030@csu.edu.cn
‡Corresponding author. E-mail: jqmeng@csu.edu.cn

© 2022 Chinese Physical Society and IOP Publishing Ltd

heated to 900 °C, and the growth end was set at 800 °C. For $TiSe_2$ and TiS_2, the temperatures are set at 800 °C and 700 °C, 700 °C, and 600 °C, respectively. For all three materials, the temperature gradient is ∼ 5 °C/cm and the iodine concentration is ∼ 5 mg/mL.

After two weeks of growth, Ti powder and chalcogenide powder can fully react to form large-size crystals. As-grown single crystals with the shiny surface are obtained, as shown in Figs. 1(a)–1(c). The crystal size of $TiTe_2$ reaches centimeters. All three crystals show different metallic lusters and have distinct 120° angles related to their crystal structure. Figure 1(d) displays the x-ray diffraction (XRD) pattern for cleaved TiX_2 single crystals. All the observed diffraction peaks can be indexed by (0,0,h) with h being an integer, indicating a pure single phase of the obtained TiX_2 single crystal. It can be found from $TiTe_2$ to $TiSe_2$ to TiS_2, the diffraction peak of the same indexed number shifts to the right. It means that the c-axis lattice constant decreases as chalcogens' ionic radius decreases. The c-axis lattice constant is calculated from XRD data, as listed in Table 1. Our results are consistent with the results reported before.[20,35]

Table 1. The chemical composition and c axis of the TiX_2 single crystals.

Crystal	Ti:X (weight%)	Ti:X (atomic)	c (Å)
$TiTe_2$	15.74 : 84.26	1 : 2.01	6.4884
$TiSe_2$	23.24 : 76.76	1 : 2.01	6.0047
TiS_2	43.28 : 56.72	1 : 1.96	5.6938

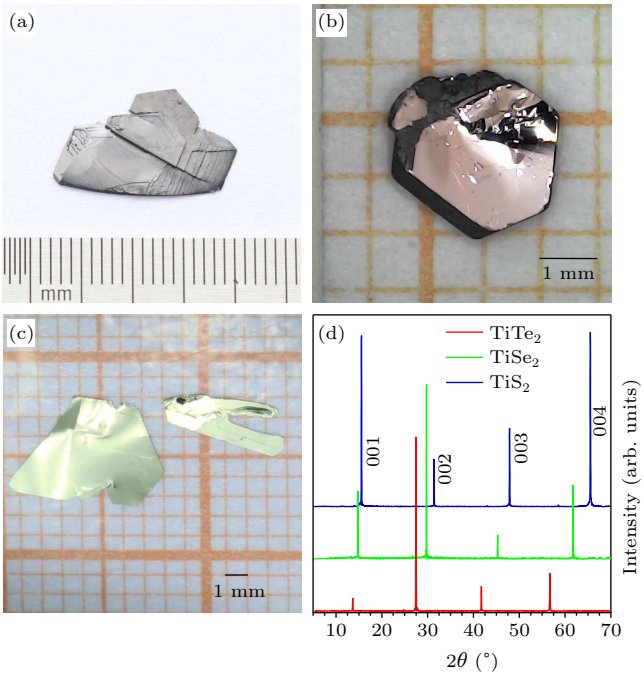


Fig. 1. (a)–(c) Photograph of the as-grown crystals of $TiTe_2$, $TiSe_2$, and TiS_2, respectively. (d) XRD patterns for cleaved single crystals of $TiTe_2$, $TiSe_2$, and TiS_2, respectively. All peaks are indexed by (0,0,h).

A scanning electron microscope (SEM) equipped with the energy dispersive spectrometer (EDS) was used to characterize the surface morphology and the chemical composition of the single crystals. Figures 2(a)–2(c) show the SEM observed smooth surfaces of $TiTe_2$, $TiSe_2$, and TiS_2, respectively. Because of their layered structure, it can be readily cleaved to get sizeable, clean, and smooth surfaces, which is necessary for surface-sensitive experiments like angle-resolved photoemission spectroscopy and scanning tunneling microscope. As shown in Fig. 2(a), the fracture between layers is usually along the edge direction.

Figure 2(d) displays a typical EDS spectrum for $TiSe_2$. The weight or atomic percentages of Ti and Se can be extracted. Table 1 summarizes the average chemical composition of TiX_2 single crystals. It can be seen that the actual atomic ratio of Ti and X in the three materials is close to 1:2, which is the ideal atomic ratio. Single-phase and accurate atomic ratios mean that we have obtained high-quality and stoichiometry TiX_2 single crystals.

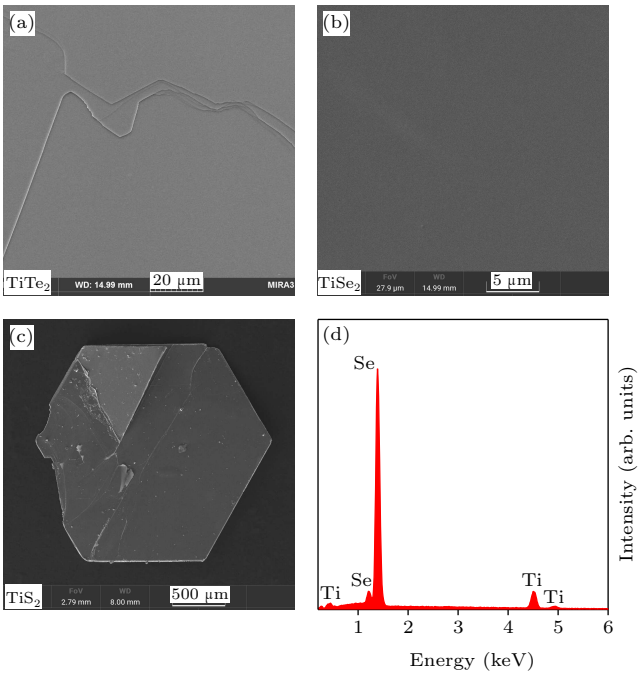


Fig. 2. (a)–(c) The surface morphology of the $TiTe_2$, $TiSe_2$, and TiS_2, respectively. (d) Typical EDS spectrum of for the single crystal $TiSe_2$. The atomic ratio of Ti : Se = 1 : 2.01.

Raman spectroscopies were used to investigate the temperature-dependent phonon behavior of TiX_2 single crystals. Raman spectroscopy on $TiTe_2$ was measured using self-built equipment in the range of 10 K–270 K, where the signal was excited by 532-nm laser and recorded by a Princeton SP2500 spectrometer equipped with a nitrogen-cooled silicon charge-coupled device camera. Raman spectroscopy (Renishaw) on $TiSe_2$ and TiS_2 single crystals were performed in the backscattering configuration under 633-nm laser excitation in the range of 80 K–300 K.

The group-theoretical analysis suggested that the layered 1T structured TiX_2 has nine vibrational modes at Γ point:[36]

$$\Gamma = E_g(2) + A_{1g} + 2A_{2u} + 2E_u(2), \quad (1)$$

where E_g and A_{1g} are Raman-active, and E_u and A_{2u} are infrared-active. The E_g and A_{1g} modes represent atomic vibrations along the *ab* plane and parallel to the *c* axis, respectively.

Figures 3(a1)–(a3) show 2D pseudocolor maps of Raman spectra of $TiTe_2$, $TiSe_2$, and TiS_2, respectively. The corresponding temperature evolution of Raman spectra of Figs. 3(a1)–(a3) at selected temperatures are displayed in Figs. 3(b1)–(b3). Several phonon modes with different strengths are observed in all three samples. These modes also behave differently with temperature.

For $TiTe_2$, five modes are observed at all temperatures [Figs. 3(a1) and 3(b1)]. At 10 K, the weak phonon modes at ~ 105 cm^{-1} (10 K) and ~ 142 cm^{-1} (10 K) are attributed to E_g and A_{1g} modes, respectively.[36–38] A peak significantly stronger than the E_g and A_{1g} modes was also observed at ~ 125 cm^{-1}, named the *M* mode and considered a zone-folded Raman-active mode.[37] However, in addition to these three phonon modes, we also observed two previously unreported modes at ~ 183 cm^{-1} (10 K) and ~ 85 cm^{-1} (10 K), respectively. Based on the existing theoretical calculations, the former phonon mode could be assigned to E_u symmetry.[36,39] Follow the same analysis as Rajaji *et al.*, the latter mode (named *K* mode) could be a Raman mode resulting from zone-folding of phonon mode from *K* or *M* of the Brillouin zone. However, it should be noted that CDW phase transition has not yet been detected in bulk $TiTe_2$, which is different from $TiSe_2$,[40] $TaSe_2$,[41] and TaS_2[42] with 1*T* structure referenced in Rajaji *et al.*'s analysis.[37] For *M* and *K* modes, further theoretical and experimental studies are necessary.

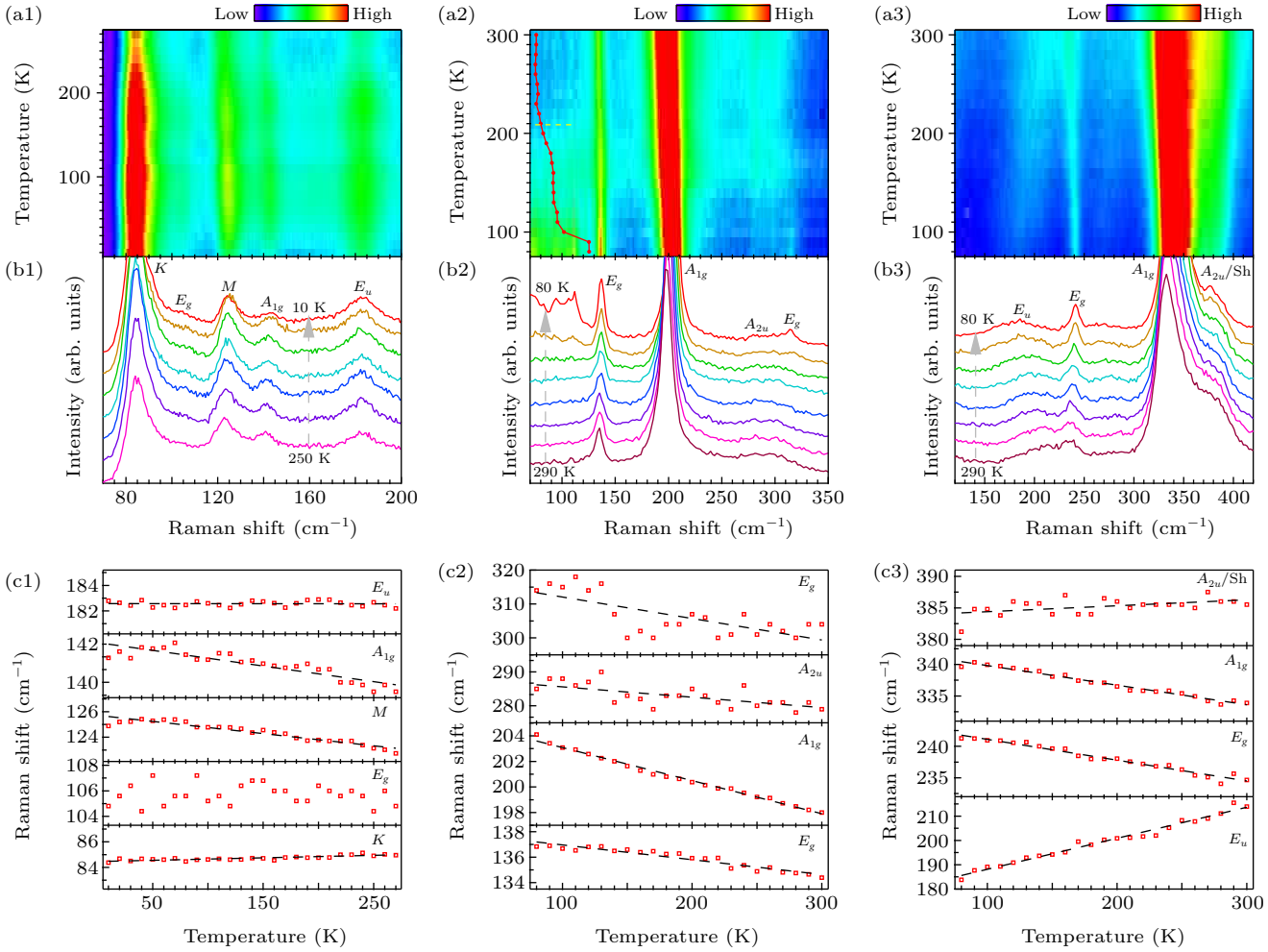


Fig. 3. (a1)–(a3) Raman intensity maps a function of Raman shift (horizontal axis) and temperature (vertical axis) for $TiTe_2$, $TiSe_2$, and TiS_2, respectively. (b1)–(b3) Corresponding Raman spectra of panels (a1)–(a3) at selected temperatures. The temperature intervals are 40, 30, and 30 K, respectively. (c1)–(c3) Temperature-dependence of Raman shift of phonon modes of $TiTe_2$, $TiSe_2$, and TiS_2, respectively. The black-dashed lines represents the result of linear fitting.

For $TiSe_2$, two strong and sharp Raman peaks at ~ 137 cm^{-1} (80 K) and ~ 204 cm^{-1} (80 K) are observed [Figs. 3(a2) and 3(b2)], which can be attributed to E_g and A_{1g} modes, respectively.[36,40,43] Other prominent features in the spectrum include broadbands at 70 cm^{-1}–115 cm^{-1} and 280 cm^{-1}–320 cm^{-1}. For the latter, the second-derivation method was used to extract the position of the phonon modes. Two modes were obtained at ~ 285 cm^{-1} (80 K) and ~ 315 cm^{-1} (80 K), respectively. The mode at ~ 285 cm^{-1} was identified as due to A_{2u}.[44] The mode at ~ 315 cm^{-1}

was assigned to E_g phonons, which was due to two-phonon processes.[40,43] However, it is not easy to distinguish the phonon mode in the broad band at 70 cm^{-1}–115 cm^{-1}. We track the change of integrated intensity with temperature in this range, showing by the red dotted line in the inset of Fig. 3(a2). It can be seen that the intensity decreases with increasing temperature, and it decreases faster around 210 K. This behavior may be related to the CDW phase transition, and similar phenomena have been reported in previous studies.[45,46] At present, there is no good explanation for the sudden change of intensity at $\sim$ 100 K, which needs further study.

As shown in Figs. 3(a3) and 3(b3), two sharp Raman peaks at $\sim$ 242 cm^{-1} (80 K) and $\sim$ 340 cm^{-1} (80 K) are observed in TiS_2, which are assigned to E_g and A_{1g} modes, respectively.[36,47,48] In addition, two significant structure features were observed, a broad peak appears at $\sim$ 185 cm^{-1} (80 K) on the low energy side of E_g peak, and a shoulder appears at $\sim$ 382 cm^{-1} (80 K) on the high energy side of the A_{1g} peak. The former mode is possibly due to the E_u mode.[36] While the latter mode has been reported,[47–51] its origin is still much debated. Researchers have proposed various possible origins, including overtone and/or summation processes,[47] excess interlayer Ti atoms,[49,52] A_{2u} symmetry,[36,51] and so on. In this work, it was noted as "A_{2u}/Sh".

We quantitatively analyze the phonons' evolution with temperatures. For phonons with distinct peaks, their positions are obtained by curve fitting. While for phonons with only the broad bands, their positions are obtained by the second-derivation. Figures 3(c1)–3(c3) show the detailed temperature dependence of positions for phonons of $TiTe_2$, $TiSe_2$, and TiS_2, respectively. The evolution of the Raman modes wavenumbers ω was fitted with a linear function

$$\omega(T) = \omega_0 + \kappa T, \tag{2}$$

where ω_0 is the phonon wavenumber for temperature extrapolated to 0 K, κ is the temperature coefficient, and T is the temperature. The fitting parameters are listed in Table 2.

Table 2. Frequency ω_0 (in unit cm^{-1}) and temperature coefficients κ (in unit cm^{-1}/K) of Raman modes of 1T-TiX_2.

Raman	$TiTe_2$		$TiSe_2$		TiS_2	
mode	ω_0	κ	ω_0	κ	ω_0	κ
E_g	105.8	–	138.1	−0.0116	244.4	−0.0331
A_{1g}	143.1	−0.0123	205.7	−0.0259	342.9	−0.0312
A_{2u}/Sh	–	–	288.6	−0.0304	383.4	0.0095
E_u	182.6	–	–	–	175.4	0.1275
M	125.7	−0.0095	–	–	–	–
K	84.5	0.0019	–	–	–	–
E_g	–	–	313.3	−0.0632	–	–

Because of the anharmonic effects, phonons usually harden as the temperature decreases, meaning that κ is a negative number. E_g and A_{1g} modes were found to harden with decreasing temperature. Because it is difficult to obtain the exact location of E_g mode of $TiTe_2$, it is not fitted here. We note that the effect of temperature on A_{1g} mode increases significantly from $TiTe_2$ to $TiSe_2$ and then TiS_2. This may be because A_{1g} mode vibrates parallel to the c axis, that the effect of temperature is opposite to the change of the c-axis lattice constant. For $TiSe_2$, the κ value for E_g mode is significantly lower than that of A_{1g} mode, which may be due to the different bonds in- and out-of-planes. In contrast, the κ value for E_g and A_{1g} modes are identical for TiS_2, which is inconsistent with the results obtained in the flake samples.[48]

We also notice some abnormal features that several phonons soften with the decrease of temperature, such as K mode of $TiTe_2$, A_{2u}/Sh and E_u modes of TiS_2. The κ value (0.0095 cm^{-1}) for the A_{2u}/Sh mode of TiS_2 is more than one order of magnitude lower than the results obtained in the flake samples (0.0592 cm^{-1}).[48] While the E_u mode of TiS_2 has a huge redshift ($\kappa = 0.1275$ cm^{-1}) with the decrease of temperature. Since the properties of some phonons, such as the A_{2u}/Sh mode, are not fully understood, further theoretical and experimental studies are needed.

Finally, we focus on the line shape of Raman spectra. Figures 4(a)–4(c) display the lowest temperature Raman spectra of $TiTe_2$, $TiSe_2$, and TiS_2, respectively. As shown in Figs. 4(b) and 4(c), the sharp Raman peaks of $TiSe_2$ and TiS_2 show good symmetry, which can be well fitted with the Lorentzian line shape. For $TiTe_2$, a striking feature is an asymmetric line shape, indicating electron–phonon (e–ph) coupling in the system. The asymmetric line shape caused by e–ph coupling can be better fitted by Fano resonance line shape[53,54]

$$I(\omega) = A\frac{[q + 2(\omega - \omega_0)/\Gamma]^2}{a + [2(\omega - \omega_0)/\Gamma]^2} + \text{baseline}, \tag{3}$$

where A, ω_0, q, and Γ are the intensity, renormalized phonon frequency in the presence of e–ph coupling, asymmetry parameter, and linewidth, respectively. Generally, $1/q$ reflects the strength of e–ph coupling. When the coupling is very weak, that is, $|1/q| \to 0$, the equation (3) reduces to the Lorentzian line shape. In Fig. 4, the solid curves are the fitted results with Eq. (3). For $TiTe_2$, the q values of K, M, and A_{1g} modes are about 4.1, 2.9, and 3.8, respectively, which means a strong e–ph coupling. For $TiSe_2$ and TiS_2, all modes have q values greater than 8, indicating weak e–ph coupling. This conclusion can also be drawn from the fact that curves can be fitted well with the Lorentzian line shape (green dashed lines). Because the laser excitation wavelengths of the three samples are different, there is no quantitative comparison of the e–ph coupling strength λ.

In conclusion, high-quality and large $TiTe_2$, $TiSe_2$, and TiS_2 single crystals have been successfully prepared by the chemical vapor transport method. XRD, SEM, and EDS characterizations demonstrate the high crystalline quality of our

sample. $TiTe_2$ phonon properties in the temperature range of 10 K to 270 K and $TiSe_2$ and TiS_2 phonon properties in the temperature range of 80 K to 300 K were measured by Raman spectroscopy. Multiple phonons were observed in all materials. In addition to the widely reported Raman modes such as E_g and A_{1g}, we also observed unreported Raman modes such as K (~ 84.5 cm^{-1}) and E_u (~ 182.5 cm^{-1}) modes for $TiTe_2$, A_{2u} mode for $TiSe_2$, and E_u mode for TiS_2. These phonons exhibit different temperature-dependent behaviors. The K mode of $TiTe_2$ and the E_u and A_{2u}/Sh modes of TiS_2 soften with temperature decreasing, while the other phonons harden with temperature decreasing . Our findings add to the understanding of TiX_2.

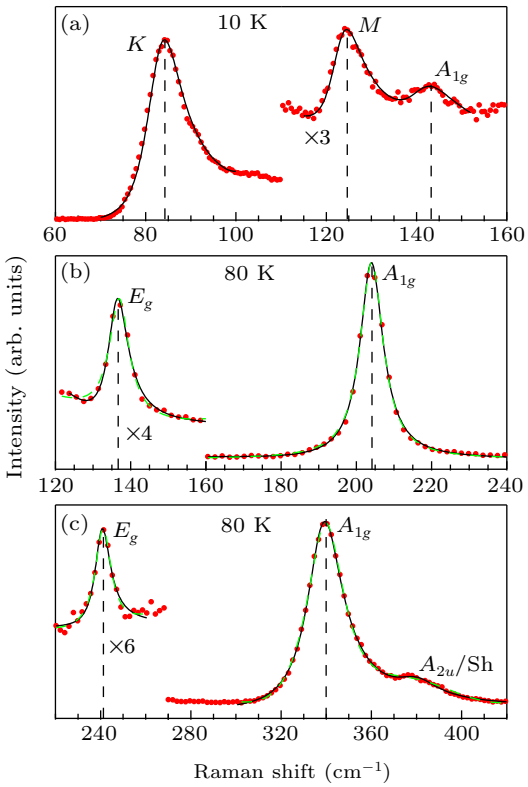


Fig. 4. (a)–(c) Low temperature Raman spectra of the $TiTe_2$, $TiSe_2$ and TiS_2, respectively. The black solid lines and green dashed lines represent the fitting results of Eq. (3) and Lorentzian line shape, respectively.

Acknowledgments

Project supported by the National Natural Science Foundation of China (Grant Nos. 12074436 and U1930116) and the Innovation-driven Plan in Central South University (Grant No. 2016CXS032).

References

[1] Hsu Y, Vaezi A, Fischer M H and Kim E 2017 *Nat. Commun.* **8** 14985
[2] Hsu Y, Cole W S, Zhang R and Sau J D 2020 *Phys. Rev. Lett.* **125** 097001
[3] Valla T, Fedorov A V, Johnson P D, Glans P, Mcguinness C, Smith K E, Andrei E Y and Berger H 2004 *Phys. Rev. Lett.* **92** 086401
[4] Chen P, Pai W W, Chan Y H, Takayama A, Xu C Z, Karn A, Hasegawa S, Chou M Y, Mo S K, Fedorov A V and Chiang T C 2017 *Nat. Commun.* **8** 516
[5] Ali M N, Xiong J, Flynn S, Tao J, Gibson Q D, Schoop L M, Liang T, Haldolaarachchige N, Hirschberger M, Ong N P and Cava R J 2014 *Nature* **514** 205
[6] Liu Y, Zhao J, Yu L, Lin C, Liang A, Hu C, Ding Y, Xu Y, He S, Zhao L, Liu G, Dong X, Zhang J, Chen C, Xu Z, Weng H, Dai X, Fang Z and Zhou X J 2015 *Chin. Phys. Lett.* **32** 67303
[7] Liu Y, Zhao J, Yu L, Lin C, Hu C, Liu D, Peng Y, Xie Z, He J, Chen C, Feng Y, Yi H, Liu X, Zhao L, He S, Liu G, Dong X, Zhang J, Chen C, Xu Z, Weng H, Dai X, Fang Z and Zhou X J 2015 *Chin. Phys. B* **24** 067401
[8] Absor M A U, Santoso I, Yamaguchi N and Ishii F 2020 *Phys. Rev. B* **101** 155410
[9] Chernozatonskii L A and Artyukh A A 2018 *Physics Uspekhi* **61** 2
[10] Naylor C H, Parkin W M, Ping J L, Gao Z L, Zhou Y R, Kim Y, Streller F, Carpick R W, Rappe A M, Drndić M, Kikkawa J M and Johnson A T C 2016 *Nano Lett.* **16** 4297
[11] Tang X F, Duan Y X, Wu F Y, Liu S Y, Zhang C, Zhao Y Z, Song J J, Luo Y, Wu Q Y, He J, Xu W and Meng J Q 2019 *Phys. Rev. B* **99** 125112
[12] Zhu S X, Zhang C, Wu Q Y, Tang X F, Liu H, Liu Z T, Luo Y, Song J J, Wu F Y, Zhao Y Z, Liu S Y, Le T, Lu X, Ma H, Liu K H, Yuan Y H, Huang H, He J, Liu H Y, Duan Y X and Meng J Q 2021 *Phys. Rev. B* **103** 115108
[13] Lin M K, Hlevyack A J, Chen P, Liu R Y, Mo S K and Chiang T C 2020 *Phys. Rev. Lett.* **125** 176405
[14] Xu S Y, Ma Q, Gao Y, Koga, Zong A, Mier V, Andrés M, Dinh T H, Huang S M, Singh B, Hsu C H, Chang T R, Ruff J P C, Watanabe K, Taniguchi T, Lin H, Karapetrov G, Xiao D, Jarillo-Herrero P and Gedik N 2020 *Nature* **578** 545
[15] Lian C, Zhang S J, Hu S Q, Guan M X and Meng S 2020 *Nat. Commun.* **11** 43
[16] Jaouen T, Rumo M, Hildebrand B, Mottas M L, Nicholson C W, Kremer G, Salzmann B, Vanini F, Barreteau C, Giannini E, Beck H, Aebi P and Monne C 2019 arXiv: 1911.06053
[17] Parvaz M, Salah N and Khan Z H 2020 *Optik* **207** 163810
[18] Ivanovskaya V V and Seifert G 2004 *Solid State Commun.* **130** 175
[19] Liu B, Yang J, Han Y H, Hu T J, Ren W B, Liu C L, Ma Y Z and Gao C X 2011 *J. Appl. Phys.* **109** 053717
[20] de Boer D K G, van Bruggen C F, Bus G W, Coehoorn R, Haas C, Sawatzky G A, Myron H W, Norman D and Padmore H 1984 *Phys. Rev. B* **29** 6797
[21] Dutta U, Malavi P S, Sahoo S, Joseph B and Karmakar S 2018 *Phys. Rev. B* **97** 060503
[22] Fragkos S, Sant R, Alvarez C, Bosak A, Tsipas P, Tsoutsou D, Okuno H, Renaud G and Dimoulas A 2019 *Adv. Mater. Interfaces* **6** 1801850
[23] Kusmartseva A F, Sipos B, Berger H, Forr O L and Tuti Ifmmode Check S Else V S Fi E 2009 *Phys. Rev. Lett.* **103** 236401
[24] Joe Y I, Chen X M, Ghaemi P, Finkelstein K D, de la Peña G A, Gan Y, Lee J C T, Yuan S, Geck J, Macdougall G J, Chiang T C, Cooper S L, Fradkin E and Abbamonte P 2014 *Nat. Phys.* **10** 421
[25] Sugawara K, Nakata Y, Shimizu R, Han P, Hitosugi T, Sato T and Takahashi T 2015 *ACS Nano* **10** 1341
[26] Chen P, ChanY H, Fang X Y, Zhang Y, Chou M Y, Mo S K, Hussain Z, Fedorov A V and Chiang T C 2015 *Nat. Commun.* **6** 8943
[27] Fang X Y, Hong H, Chen P and Chiang T C 2017 *Phys. Rev. B* **95** 201409
[28] Calandra M and Mauri F 2011 *Phys. Rev. Lett.* **106** 196406
[29] Hedayat H, Sayers C J, Bugini D, Dallera C, Wolverson D, Batten T, Karbassi S, Friedemann S, Cerullo G, van Wezel J, Clark S R, Carpene E and Da E C 2019 *Phys. Rev. Research* **1** 023029
[30] Liao J, Zhao Y, Zhao Y, Yang X and Chen Y 2020 *J. Appl. Phys.* **127** 044301
[31] Zhang M, Wang X, Rahman A, Zeng Q, Huang D, Dai R, Wang Z and Zhang Z 2018 *Appl. Phys. Lett.* **112** 041907
[32] Liu W, Luo A, Zhong G, Zou J and Xu G 2021 arXiv: 2105.01328v1
[33] Zhu Z Y, Cheng Y and Schwingenschlögl U 2015 *Sci. Rep.* **4** 4025
[34] Liu S Y, Zhu S X, Wu Q Y, Zhang C, Song P B, Shi Y G, Liu H, Liu Z T, Song J J, Wu F Y, Zhao Y Z, Tang X F, Yuan Y H, Huang H, He J, Liu H Y, Duan Y X and Meng J Q 2021 *Results in Physics* **30** 104816
[35] Al-Alamy F A S and Balchin A A 1977 *J. Cryst. Growth* **38** 221
[36] Ding H and Xu B 2012 *J. Chem. Phys.* **137** 224509
[37] Rajaji V, Dutta U, Sreeparvathy P C, Sarma S C, Sorb Y A, Joseph B, Sahoo S, Peter S C, Kanchana V and Narayana C 2018 *Phys. Rev. B* **97** 085107
[38] Hangyo M, Nakashima S and Mitsuishi A 1983 *Ferroelectrics* **52** 151

[39] Xiao R C, Lu W J, Shao D F, Li J Y, Wei M J, Lv H Y, Tong P, Zhu X B and Sun Y P 2017 *J. Mater. Chem. C* **5** 4167
[40] Goli P, Khan J, Wickramaratne D, Lake R K and Balandin A A 2012 *Nano Lett.* **12** 5941
[41] Samnakay R, Wickramaratne D, Pope T R, Lake R K, Salguero T T and Balandin A A 2015 *Nano Lett.* **15** 2965
[42] Albertini O R, Zhao R, Mccann R L, Feng S, Terrones M, Freericks J K, Robinson J A and Liu A Y 2016 *Phys. Rev. B* **93** 214109
[43] Holy J A, Woo K C, Klein M V and Brown F C 1977 *Phys. Rev. B* **16** 3628
[44] Catlow C R A and Kotomin E A 2003 *Computational Materials Science* (Amsterdam: IOS Press)
[45] Wang H, Chen Y, Duchamp M, Zeng Q, Wang X, Tsang S H, Li H, Jing L, Yu T, Teo E H T and Liu Z 2018 *Adv. Mater.* **30** 1704382
[46] Snow C S, Karpus J F, Cooper S L, Kidd T E and Chiang T C 2003 *Phys. Rev. Lett.* **91** 136402
[47] Sandoval S J, Chen X K and Irwin J C 1992 *Phys. Rev. B* **45** 14347
[48] Dużyńska A, Judek J, Wilczyński K, Zberecki K, Łapińska A, Wróblewska A and Zdrojek M 2019 *J. Raman Spectrosc.* **50** 1
[49] Sherrell P C, Sharda K, Grotta C, Ranalli J, Sokolikova M S, Pesci F M, Palczynski P, Bemmer V L and Mattevi C 2018 *ACS Omega* **3** 8655
[50] Lin C, Zhu X, Feng J, Wu C, Hu S, Peng J, Guo Y, Peng L, Zhao J, Huang J, Yang J and Xie Y 2013 *J. Am. Chem. Soc.* **135** 5144
[51] Vaterlaus H P and Levy F 1985 *J. Phys. C: Solid State Phys.* **18** 2351
[52] Klipstein P C, Bagnall A G, Liang W Y, Marseglia E A and Friend R H 1981 *J. Phys. C: Solid State Phys.* **14** 4067
[53] Klein M V 1982 *Light Scattering in Solids, Topics in Applied Physics*, 2nd ed. (Berlin: Springer)
[54] Wu S F, Richard P, Wang X B, Lian C S, Nie S M, Wang J T, Wang N L and Ding H 2014 *Phys. Rev. B* **90** 054519